Fibroblasts from patients with idiopathic pulmonary fibrosis are resistant to cisplatin-induced cell death via enhanced CK2-dependent XRCC1 activity

Jintaek Im[1] · Richard Seonghun Nho[1]

Abstract

Idiopathic pulmonary fibrosis (IPF) is a deadly and progressive fibrotic lung disease, but the precise etiology remains elusive. IPF is characterized by the presence of apoptosis-resistant (myo)fibroblasts that relentlessly produce a collagen-rich extracellular matrix (ECM). Recent studies showed that an anti-cancer chemotherapy drug cisplatin is implicated in the development of pulmonary fibrosis, suggesting that the treatment of cancer patients with cisplatin may alter fibroblast viability. To address this possibility, we investigated the cisplatin-induced cell death mechanism in lung fibroblasts derived from IPF and non-IPF patients in response to a collagen matrix. IPF fibroblasts showed enhanced resistance to cisplatin-induced cell death compared to non-IPF fibroblasts in a time- and dose-dependent manner. Molecular study showed that the expression of γH2AX, PUMA and caspase-3/7 activity was abnormally reduced in IPF fibroblasts, suggesting that DNA damage-induced apoptosis caused by cisplatin was suppressed in IPF fibroblasts. Our study further revealed that DNA repair protein XRCC1 activity was aberrantly increased as a result of CK2 hyper-activation in cisplatin-treated IPF fibroblasts, and this alteration protected IPF fibroblasts from cisplatin-induced cell death. Our results showed that IPF fibroblasts residing in a collagen rich matrix are resistance to cisplatin-induced cell death due to the aberrantly high CK2/XRCC1-dependent DNA repair activity. This finding suggests that pulmonary fibrosis may develop and worsen due to the presence of apoptosis-resistant lung fibroblasts in cisplatin-treated cancer patients.

Keywords IPF · Apoptosis · Cisplatin · Lung fibroblasts

Introduction

IPF is a lethal and irreversible lung disease that the precise etiology is unknown [1–3]. IPF is characterized by excessive accumulation of collagen rich extracellular matrix and the presence of apoptosis-resistant (myo)fibroblasts [4, 5]. When normal lung fibroblasts interact with a type I fibrillar collagen matrix, they undergo apoptosis [6–8], which prevents excessive fibro-proliferation after tissue injury [4, 9]. In contrast, IPF fibroblasts elude collagen matrix-driven apoptosis, promoting lung fibrosis [6, 8, 10]. Recent studies revealed that IPF fibroblasts interacted with a collagen matrix

maintain an apoptosis-resistant phenotype in response to various cell death-inducing insults [6, 8, 10–12]. IPF fibroblasts suppress cell cycle inhibitor and apoptosis-inducing protein FoxO3a to maintain a pathological phenotype on collagen as a result of aberrant PI3K/Akt activation [12, 13]. IPF fibroblasts are also known to up-regulate BRCA2 and RAD51, thereby protecting them from ionizing radiation-induced cell death [11]. These findings suggest that IPF fibroblasts utilize multiple mechanisms that effectively protect them from various apoptosis-inducing environments. Cis-diamminedichloroplatinum (II) (cisplatin) is a potent antitumor agent and has been used for the treatment of ovarian, cervical, breast, bladder and lung cancers [14, 15]. Cisplatin interferes with DNA replication, increasing DNA damage mainly by forming Pt-d(GpG), which promotes cancer cell death [16]. However, in spite of cisplatin's established effects for the treatment of cancers, there has been a growing concern that cancer patients have an increased risk of developing lung fibrosis due to cisplatin-induced toxicity

✉ Richard Seonghun Nho
nhoxx002@umn.edu

1 Department of Medicine, University of Minnesota, 420 Delaware Street SE., Box 276, Minneapolis, MN 55455, USA

[17–19]. Cisplatin is known to cause renal tubulointerstitial and pulmonary fibrosis in humans [19]. A prior study also showed that chemotherapy with cisplatin or in combination with other cytotoxic agents is correlated with increase in pulmonary fibrosis [20]. These studies indicate a possibility that the treatment of cancer patients with cisplatin triggers the fibrotic process by the activation of fibroblasts that are resistant to DNA damage. However, it is not clear whether IPF fibroblasts evade cisplatin-induced apoptosis via increasing DNA repair activity, which causes them to maintain a pathological phenotype. To test this, we investigated the molecular mechanism that underlies cisplatin resistance in fibroblasts derived from patients with IPF. Unlike non-IPF fibroblasts, IPF fibroblasts were more resistant to cisplatin-induced cell death on collagen. To support this finding, reduced DNA damage was mainly found in cisplatin-treated IPF fibroblasts, indicating that the mechanism to repair damaged DNA is abnormally activated in IPF fibroblasts. We showed that DNA repair protein X-ray repair cross-complementing protein 1 (XRCC1) activity was increased in IPF fibroblasts in response to cisplatin. Our study further revealed that abnormally high casein kinase 2 (CK2) activity increased XRCC1 function, which subsequently protected IPF fibroblasts from cisplatin-induced apoptosis by increasing DNA repair. Our results suggest that cisplatin for cancer treatment may increase the risk of developing lung fibrosis due to the presence of fibrotic fibroblasts that are resistant to DNA damage. We propose that cisplatin may be carefully used for cancer patients who have signs of lung fibrosis.

Materials and methods

Human subjects and the isolation of primary lung fibroblasts

Lung tissues removed at the time of transplantation or death from non-IPF and IPF patients (n = 8, each). The tissue samples were stripped of all identifiers and designated as waste (exemption 4). Written informed consent was obtained on all patients prior to the procedure being performed. Use of human lung tissues was approved by the Institutional Review Board (IRB) at the University of Minnesota. The diagnosis of IPF was supported by history, physical examination, pulmonary function tests, and typical high-resolution chest computed tomographic findings of IPF. In all cases, the diagnosis of IPF was confirmed by microscopic analysis of lung tissues that demonstrated the characteristic morphological findings of interstitial pneumonia [2, 5]. Lung fibroblasts from non-IPF donors were used as control fibroblasts. For the preparation of IPF and control lung fibroblasts, removed lung tissues were chopped to 5 mm^3 and cultured in Dulbecco's modified Eagle's medium (DMEM; MilliporeSigma, St.

Louis, MO, USA) supplemented with 20% fetal calf serum (FCS; HyClone, Logan, UT, USA) and 2% antibiotics for 4–5 weeks at 37 °C in a 5% CO_2 humidified incubator. All isolated fibroblasts with low passage numbers (less than 9) were used for this study.

Collagen matrix preparation

Collagen matrix was prepared using 80% of type I collagen solution (Advanced Biomatrix, San Diego, CA, USA), 10% 10× DMEM and 10% 1× DMEM, and the pH was adjusted to 7.2 with 0.1 M NaOH. Cell culture dishes or 96 well plates were coated with type I collagen and incubated for a minimum of 2 h at 37 °C prior to use. After incubation in serum free (SF) DMEM for an additional 24 h, cells were treated with cis-Diammineplatinum (II) dichloride (cisplatin; MilliporeSigma) for the indicated time periods. Dimethyl sulfoxide (DMSO; MilliporeSigma) was used as a vehicle control (VH) for all experiments.

Chemical inhibitor, siRNA and XRCC1 expression vector

IPF fibroblasts on collagen matrix (n = 4) were treated with a 10 μM CK2 inhibitor, 2-dimethylamino-4, 5, 6, 7-tetrabromobenzimidazole (DMAT) for 1 h prior to cisplatin treatment. For silencing, IPF fibroblasts (n = 4) were transfected with 50 nM XRCC1, or CK2 siRNA (catalog No. SC-36859, or SC-29918; Santa Cruz Biotechnology) using Lipofectamin RNAiMAX (Life Technologies, Carlsbad, CA). Scrambled siRNA was used as a control (catalog No. SC-37007). For the overexpression of XRCC1, control fibroblasts (n = 4) were transfected with a XRCC1-pCMV6 vector (Addgene, Canbridge, MA) using Lipofectamin 3000 (Life technologies) in OPTI MEM media. Empty vector pCMV6 transfected cells were used as a control. For the elucidation of the role of CK2 that regulates XRCC1 functions, CK2 silenced IPF fibroblasts (n = 4) were transfected with a XRCC1-pCMV6 vector, and incubated for 24 h. Cells were then plated on collagen matrices in SF DMEM for an additional 24 h followed by the treatment of control and IPF cells with 100 μM cisplatin for various time points.

Western blot analysis and antibodies

Control and IPF fibroblasts (n = 8, each) used for cell viability assay (6 × 10^5 cells/60 mm cell culture dish) were treated with cisplatin for various time points. Cells were lysed with 1× cell lysis buffer (Cell Signaling technology, Beverly, MA) containing protease inhibitor (Roche Applied Science, Indianapolis, IN) and phosphatase inhibitor (Research Products International Corp., Mount Prospect, IL), and western blotting was performed as previously described [15–17].

The antibodies used for our study are: γH2AX (PRID: AB_2118009, Cell Signaling Technology) [21], H2AX (RRID: AB_10694556, Cell Signaling technology) [22], RAD51 (RRID: AB_2042762, Abcam, Cambridge, UK) [11], BRCA2 (RRID: AB_2259370; R&D systems, Minneapolis, MN) [11], pXRCC1 (phosphorylated at S518, T519, and T523; catalog No. ab195205; Abcam) [21], XRCC1 (RRID:AB_10985840; ThermoFisher Scientific, Pittsburgh, PA) [23], CK2α (catalog No. 2656; Cell Signaling technology) [24], PUMA (RRID:AB_10987708; Santa Cruz Biotechnology, Santa Cruz, CA) [25], or GAPDH (RRID:AB_627679; Santa Cruz Biotechnology) [26]. The protein bands on a membrane were then detected by ECL solution (ThermoFisher Scientific) using Chemi Doc-IT2 image analyzer (UVP BioImage systems, Upland, CA), and quantified using VisionWorks LS program (UVP BioImage systems).

Cell viability, caspase 3,7 and CK2 activity assay

Randomly selected 8 control and 8 IPF fibroblasts (1×10^4 cells/well of a 96 well plate) were cultured in the presence or absence of a type I collagen matrix under the aforementioned conditions. After the cisplatin treatment, cells were incubated with 20 μL of Cell Titer Blue reagent (Promega, Madison, WI) for 3 h, and cell viability was measured at 560 nm (Ex)/590 nm (Em) of fluorescence using a 96-well plate reader (BioTek, Winooski, VT). Caspase 3/7 activity was measured using Apo-ONE Homogeneous caspase-3/7 assay kit (Promega). Briefly, same control and IPF fibroblasts (n = 8, each) used in cell viability assay were cultured on a 96 well plate pre-coated with a type I collagen matrix in serum free DMEM for 24 h. The cells were then treated with DMSO (VH) or cisplatin and incubated for an additional 12 h. Cells were then incubated with 50 μL of diluted caspase substrate in caspase-3/7 buffer for 1 h at room temperature on a shaker. Caspase 3/7 activity was measured at 499 nm (Ex)/521 nm (Em) of fluorescence using a 96-well plate reader (BioTek). CK2 activity was measured using CycLex CK2 Kinase Assay/Inhibitor Screening kit (MBL International Corp., Woburn, MA) according to manufacturer's instructions. Briefly, same control and IPF fibroblasts (n = 8, each) used in cell viability assay were cultured on a 60 mm cell culture dish pre-coated with a collagen matrix in SF DMEM for 24 h. The cells were then treated with DMSO (VH) or 100 μM cisplatin and incubated for an additional 12 h. Cells were then detached using collagenase (5 mg/mL DMEM, ThermoFisher Scientific) and harvested by centrifugation at 300×g for 5 min. The cell pellets were lysed by sonication for 40 s on ice and collected by centrifugation. 50 μL lysates were seeded on a 96 well plate and incubated with 90 μL of kinase reaction buffer containing ATP for 30 min at 37 °C. After the incubation, the plate

were incubated with 100 μL of HRP conjugated antibody and substrate reagent for 30 min. CK2 activity was measured at 450 nm/540 nm using a 96-well plate reader (BioTek).

Statistics

Data are expressed as the means ± SEM. Box-and whisker showing lowest, lower quartile, median, upper quartile and highest viability and dot plots were created by Prism V7.0 (GraphPad Software, La Jolla, CA, USA). Two-way ANOVA was used for the analysis of fibroblast viability through Prism V7.0. Two-dimensional column graphs were prepared using Microsoft Excel. Protein levels between DMSO (VH) and cisplatin treated fibroblasts or cisplatin treated IPF and control fibroblasts were analyzed using two-tailed Student's t-test. Significance level was set at $p < 0.05$.

Results

IPF fibroblasts are resistant to cisplatin-induced cell death

Studies showed that lung fibroblasts derived from IPF patients maintain an apoptosis-resistant phenotype in response to a collagen matrix, participating in developing lung fibrosis [11–13]. Cisplatin is implicated in promoting lung fibrosis, which indicates that IPF fibroblasts cultured on a collagen matrix are resistant to cisplatin-induced cell death. To test this, we first treated non-IPF and IPF fibroblasts (n = 8 each) with various doses of cisplatin, and their viability was measured. Enhanced viability was mainly found in IPF fibroblasts compared to that of control fibroblasts in response to various doses of cisplatin (Fig. 1a). Time course assay further showed that IPF fibroblasts were significantly more viable after cisplatin treatment compared to control fibroblasts (Fig. 1b). These results suggested that IPF fibroblasts primarily utilize a mechanism to elude cisplatin-induced cell death.

DNA damage is reduced in IPF fibroblasts in response to cisplatin

Cisplatin is a chemotherapy drug to induce inter and intra-strand DNA crosslinks, which promotes DNA damage [14]. γH2AX is a DNA damage marker protein [27–29], and H2AX phosphorylation occurs in response to cisplatin-induced DNA lesions [27]. Therefore, we measured γH2AX levels to examine whether reduced DNA damage is responsible for the enhanced resistance of IPF fibroblasts against cisplatin. γH2AX expression was progressively increased in cisplatin treated control fibroblasts while reduced γ-H2AX expression was found in IPF fibroblasts as a function of
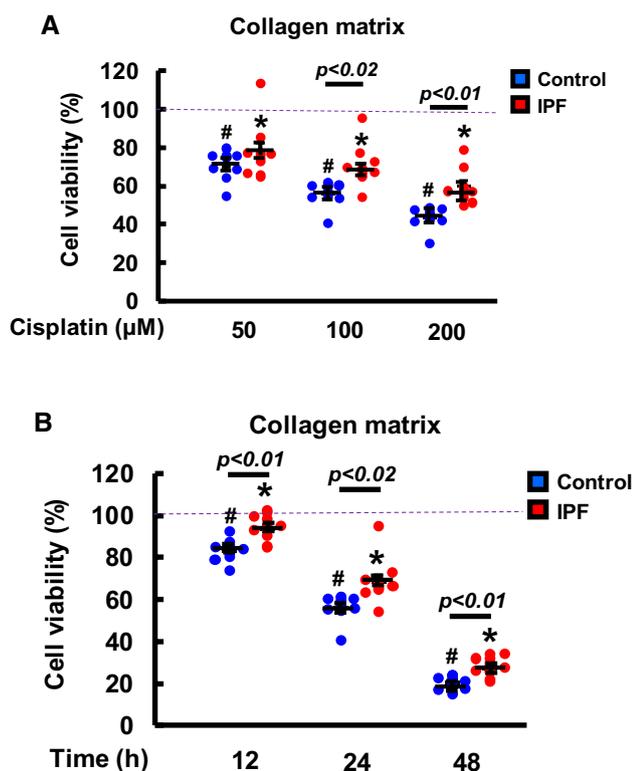
A

Collagen matrix

B

Collagen matrix

Fig. 1 IPF fibroblasts are resistant to cisplatin-induced cell death on collagen. **a** Cell viability of control and IPF fibroblasts (n = 8, each) treated with various doses (50–200 μM) of cisplatin on a collagen matrix at 24 h. **b** Cell viability of control and IPF fibroblasts (n = 8, each) cultured on a collagen matrix at various time points in the presence of 100 μM of cisplatin. DMSO was used as a vehicle control (VH). Each blue and red dot represents the viability of individual control and IPF fibroblast, respectively. Values are presented in mean ± SEM of percentages of fibroblast viability compared to vehicle control treated control and IPF fibroblasts set at 100% (a dotted line). Two-way ANOVA was used for the analysis of fibroblast viability. #, *Indicate the statistical significance of control or IPF fibroblast viability compared to DMSO treated control or IPF cells, respectively. $p < 0.05$. Statistical significance between control and IPF fibroblasts in response to various doses of cisplatin or at various time points is also shown

time (Fig. 2a, left). Statistical analysis further demonstrated that γ-H2AX/H2AX expression was fivefold decreased in IPF fibroblasts compared to that of control fibroblasts at 24 h (Fig. 2a, right). DNA damage by cisplatin is known to promote cell death via the activation of pro-apoptotic proteins PUMA, caspase 3 and 7 [30]. To further test whether enhanced IPF fibroblast viability in response to cisplatin is due to the reduced apoptosis, the expression and activity of these proteins in cisplatin treated control and IPF fibroblasts were measured. PUMA expression remained rather unaltered in IPF fibroblasts compared to the levels in control fibroblasts at various time points (Fig. 2b, left and right). Similar to this finding, caspase 3/7 activity also remained low in IPF fibroblasts while control fibroblasts showed

enhanced caspase-3/7 activity in the presence of cisplatin (Fig. 2c). These results showed that DNA damage-induced apoptosis was aberrantly low in IPF fibroblasts in response to cisplatin.

Abnormally high XRCC1 activity protects IPF fibroblasts from cisplatin-induced apoptosis

Cisplatin causes DNA damage, and the abnormal activation of XRCC1 is known to protect cancer cells from cisplatin-induced apoptosis [31–33]. XRCC1 activity is regulated by phosphorylation, and this event is dependent upon CK2 activation [32, 34, 35]. To test whether enhanced XRCC1 suppresses DNA damage-induced apoptosis via CK2, we next examined XRCC1 expression and its activity in cisplatin treated control and IPF fibroblasts on collagen. Total XRCC1 expression remained relatively unaltered in control and IPF fibroblasts at various time points (Fig. 3a, left and right). However, phosphorylated XRCC1 was predominantly increased in cisplatin treated IPF fibroblasts as a function of time. p-XRCC1/XRCC1 expression demonstrated that the activation of XRCC1 was mainly found in cisplatin-treated IPF fibroblasts (Fig. 3a, lower). We further examined the possibility that DNA repair proteins other than XRCC1 also protect IPF fibroblasts from cisplatin-induced DNA damage. BRCA2 and RA51 are associated with DNA break repair, and when IPF fibroblasts are exposed to ionizing radiation, these proteins are abnormally increased, protecting them from radiation-induced cell death [11]. Time course assay showed that there was no statistically significant difference in BRCA2 and RAD51 expression between control and IPF fibroblasts (Fig. 3b). These results suggested that enhanced XRCC1 activity that repairs damaged DNA is the major mechanism in IPF fibroblasts to maintain a viable phenotype against cisplatin.

To further test whether the hyper-activation of XRCC1 causes resistance of IPF fibroblasts to cisplatin-induced cell death, we next silenced XRCC1 protein, and DNA damage and fibroblast viability were measured. When IPF fibroblasts treated with XRCC1 siRNA were cultured on collagen in the presence of cisplatin, γH2AX levels were highly increased (Fig. 3c, upper, lane 4). γH2AX/H2AX expression further demonstrated that there was about fourfold increase in DNA damage in XRCC1 silenced IPF fibroblasts compared to that of scramble siRNA treated cells (Fig. 3c, lower). To support the anti-apoptotic role of XRCC1, the viability of XRCC silenced IPF fibroblasts was also decreased compared to that of non-functional siRNA treated fibroblasts (Fig. 3d, blue and red boxes). These results showed that abnormally high XRCC1 activity repairs damaged DNA, which subsequently protects IPF fibroblasts from cisplatin-induced cell death.
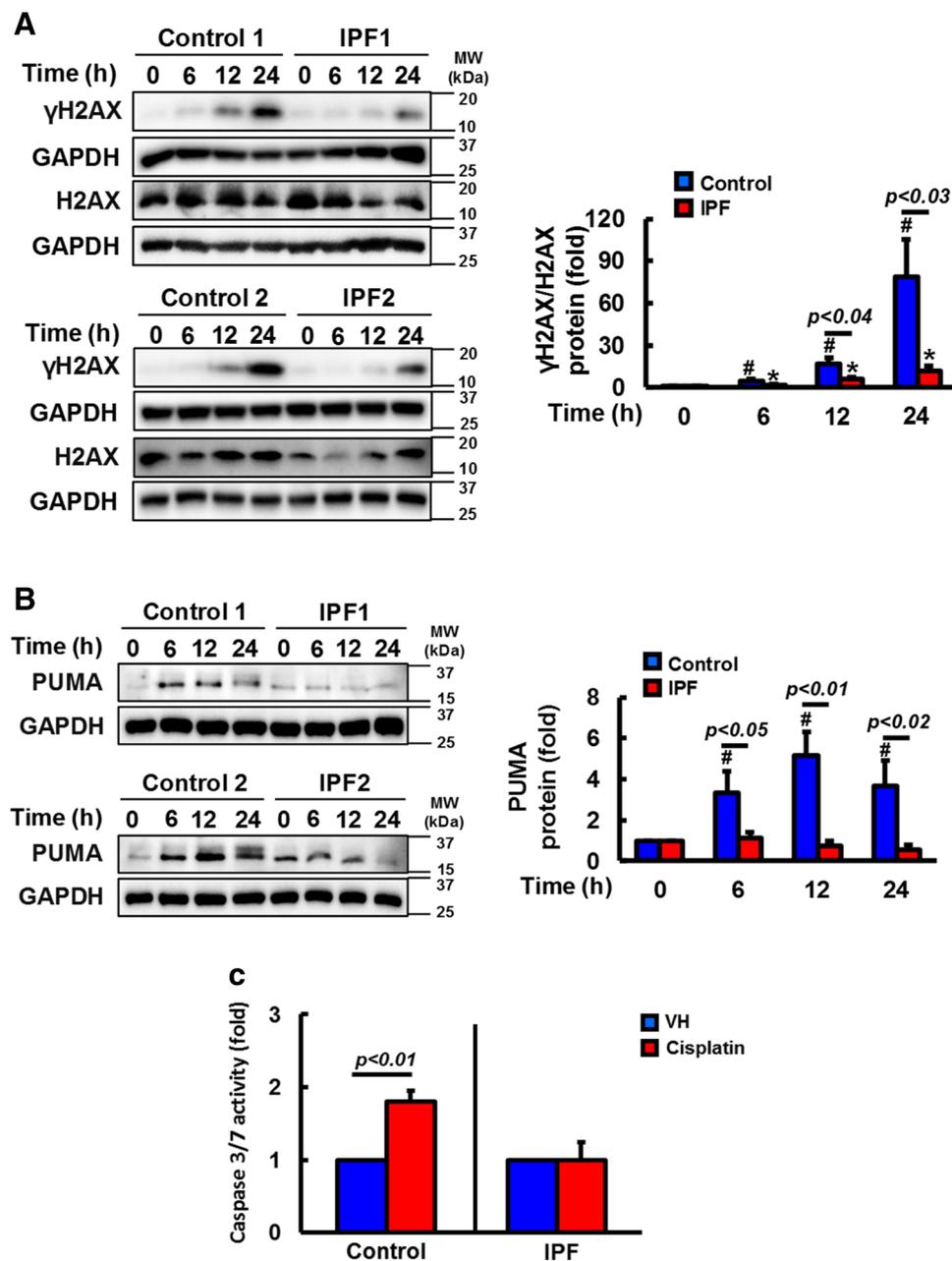
Fig. 2 Cisplatin treated IPF fibroblasts on collagen show reduced DNA damage and apoptosis. **a** *Left*, representative γH2AX and total H2AX protein expression in randomly selected control and IPF fibroblasts (n = 8, each) on collagen as a function of time in the presence of 100 μM of cisplatin. GAPDH was used as a loading control. DMSO was used as a vehicle control. *Right*, statistical analysis of γH2AX/H2AX expression in cisplatin treated control and IPF fibroblasts (n = 8, each) as a function of time. Values are presented in mean ± SEM of fold changes of γH2AX/H2AX expression. #, *Indicate the statistical significance of γH2AX/H2AX expression in control or IPF fibroblasts at various time points compared to control or IPF cells at 0 h, respectively. $p < 0.05$. **b** *Left*, representative PUMA protein expression in control and IPF fibroblasts (n = 8, each) as a function of time in response to 100 μM cisplatin on collagen. *Right*, statistical analysis of PUMA expression in cisplatin treated control and IPF fibroblasts (n = 8, each) as a function of time. #Indicates the statistical significance of PUMA expression in control fibroblasts at various time points compared to control cells at 0 h. $p < 0.05$. **c** Shown is the caspase 3/7 activity in control or IPF fibroblasts (n = 8, each) cultured on collagen in the presence of 100 μM cisplatin at 12 h. DMSO was used as a control (VH). Values are presented in mean ± SEM of fold changes of caspase activity compared to VH treated control or IPF fibroblasts set at onefold. Numerical p value indicates statistical significance between VH and cisplatin treated control fibroblasts
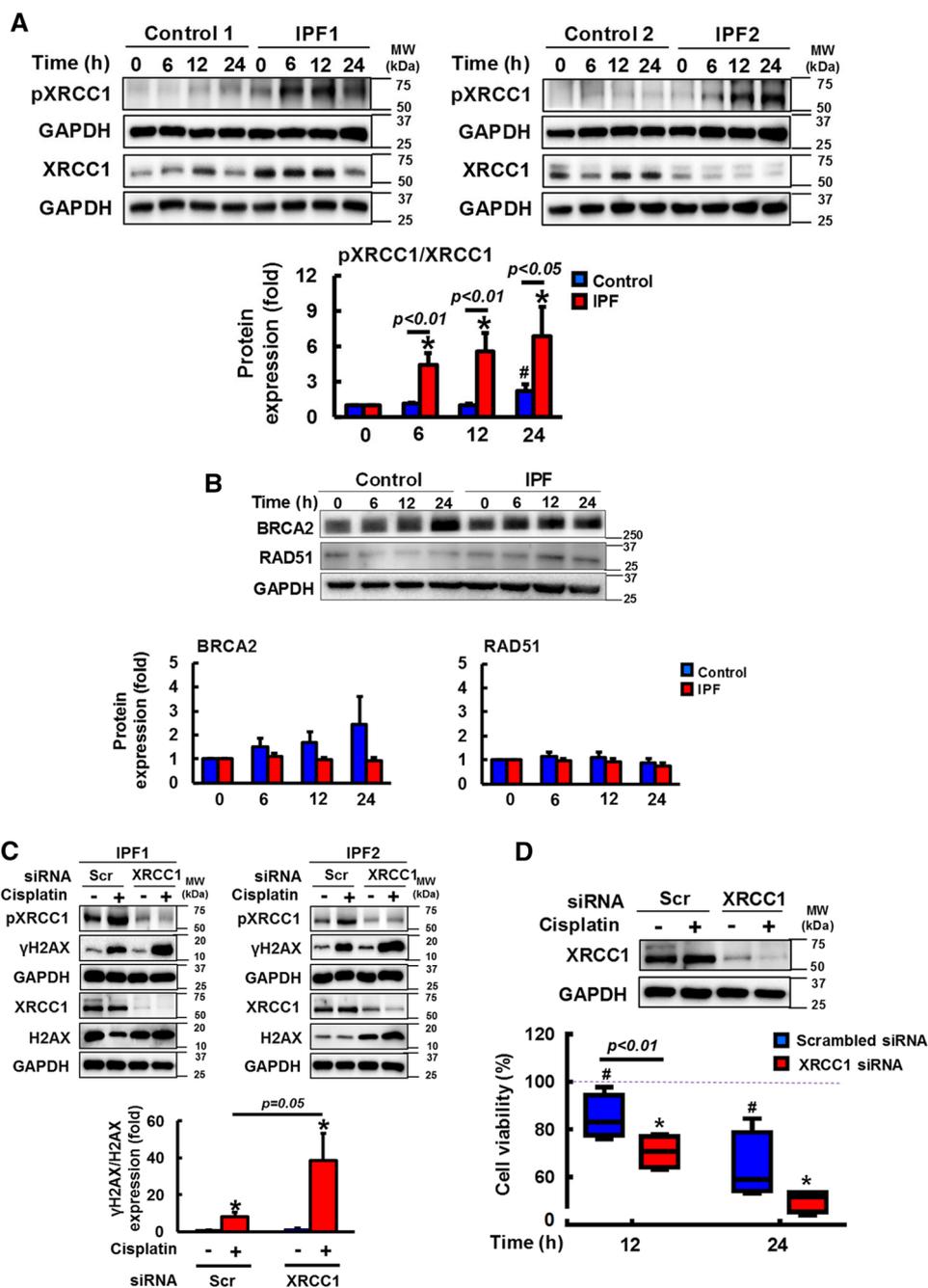
CK2 activation suppresses DNA damages, reducing the cytotoxic effects of cisplatin in IPF fibroblasts

CK2 is known to stabilize XRCC1 protein, increasing its function, which promotes DNA repair activity [32, 34, 35]. Our results shown in Fig. 3 suggested that CK2 becomes activated when IPF fibroblasts are treated with cisplatin, which protects IPF fibroblasts from cisplatin-induced DNA damage via XRCC1 activation. To test this, we next measured CK2 activity in control and IPF fibroblasts in the presence or absence of cisplatin on collagen. CK2 activity was significantly increased in cisplatin treated IPF fibroblasts while no noticeable changes in CK2 activity were found in control fibroblasts in the presence or absence of cisplatin (Fig. 4a). To further test this, IPF fibroblasts were treated with a CK2 inhibitor DMAT, and CK2 activity was measured in the presence or absence of cisplatin. CK2 activity was highly increased in the absence of DMAT while the activity of CK2 remained low in DMAT treated IPF fibroblasts in the presence of cisplatin (Fig. 4b). These findings further suggested that CK2 becomes abnormally activated when IPF fibroblasts are treated with cisplatin

◀**Fig. 3** Apoptosis-resistant IPF fibroblasts against cisplatin is due to abnormal XRCC1 activation. **a** *Upper*, representative pXRCC1 and total XRCC1 protein expression in randomly selected control (n = 8) and IPF (n = 8) fibroblasts cultured on collagen in the presence of 100 μM cisplatin at various time points. *Lower*, statistical analysis of pXRCC1/XRCC1 expression in control and IPF fibroblasts under the same condition. Values are presented in mean ± SEM of fold changes of pXRCC1/XRCC1 expression at various time points compared to DMSO treated control or IPF fibroblasts set at onefold. #, *Indicate the statistical significance of p-XRCC1/XRCC1 expression in control and IPF fibroblasts compared to control and IPF cells at 0 h, respectively. $p < 0.05$. Numerical p values indicate statistical significance between control and IPF fibroblasts. **b** *Upper*, representative BRCA2 and RAD51 protein expression in randomly selected control and IPF fibroblasts (n = 8, each) on collagen as a function of time in the presence of 100 μM cisplatin. GAPDH was used as a loading control. DMSO was used as a vehicle control (VH). *Lower*, statistical analysis of BRCA2 and RAD51 expression in control and IPF fibroblasts under the same condition. Values are presented in mean ± SEM of fold changes of BRCA2 or RAD51 compared to DMSO treated control or IPF fibroblasts at 0 h set at onefold. **c** *Upper*, representative γH2AX, total H2AX, pXRCC1, and total XRCC1 protein expression in XRCC1 silenced IPF fibroblasts (n = 4) at 12 h in the presence or absence of 100 μM cisplatin on collagen. *Lower*, statistical analysis of γH2AX/H2AX protein levels normalized to GAPDH in IPF fibroblasts transfected with scrambled (Scr) or XRCC1 siRNA in the presence or absence of cisplatin. Values are presented in mean ± SEM of fold changes of γH2AX/H2AX. *Indicates the statistical significance of γH2AX/H2AX expression in Scr or XRCC1 siRNA treated IPF fibroblasts compared to DMSO treated cells. γH2AX/H2AX expression in DMSO treated, Scr siRNA transfected IPF fibroblasts set at onefold. **d** *Upper*, XRCC1 protein levels in IPF fibroblasts transfected with Scr or XRCC1 siRNA in the presence or absence of cisplatin on collagen at 12 h. *Lower*, changes of cell viability in XRCC1 silenced IPF fibroblasts (n = 4) on collagen at 12 and 24 h in response to 100 μM cisplatin. Values are presented in mean ± SEM of percentages of viability. IPF fibroblasts treated with DMSO and Scr siRNA set at 100%. # or *Indicates the statistical significance of cell viability of IPF fibroblasts transfected with Scr or XRCC1 siRNA at 12 and 24 h in the presence of cisplatin compared to DMSO and Scr siRNA treated IPF cells at 0 h, respectively. $p < 0.05$

on collagen. To test whether enhanced CK2 repairs DNA damage via XRCC1 activation, we next measured γH2AX levels in control and IPF fibroblasts in the presence of DMAT. Unlike control fibroblasts, γH2AX/H2AX expression was highly increased in DMAT-treated IPF fibroblasts in response to cisplatin (Fig. 4c, upper lane 8, and lower). In contrast, p-XRCC1/XRCC1 levels were reduced in IPF fibroblasts while p-XRCC1/XRCC1 levels remained low and relatively unaltered in control fibroblasts under the same condition (Fig. 4c, upper and lower right). These findings indicated that abnormally high CK2 activity increases DNA repair in IPF fibroblasts, protecting them from cisplatin-induced cell death. To confirm this, we next silenced CK2 in IPF fibroblasts, and γH2AX, H2AX, p-XRCC1

and XRCC1 expression levels were measured. Similar to the prior results, CK2 silencing in IPF fibroblasts highly increased γH2AX levels while p-XRCC1 levels remained low (Fig. 4d, upper lane 4). γH2AX/H2AX and p-XRCC-1/XRCC1 levels further showed that the inhibition of CK2 suppressed XRCC1 activity and promoted DNA damage in IPF fibroblasts (Fig. 4d, lower). These results strongly suggested that the abnormally activated CK2/XRCC1 axis confers apoptosis-resistant IPF fibroblasts against cisplatin. In support of these findings, the viability of IPF fibroblasts treated with CK2 siRNA was also significantly decreased at 12 and 24 h compared to that of IPF fibroblasts treated with scramble siRNA in response to cisplatin (Fig. 4e, lower). Collectively, our results showed that CK2 activity is aberrantly up-regulated in cisplatin-treated IPF fibroblasts, and that this alteration increases DNA repair, subsequently protecting IPF fibroblasts from cisplatin-induced cell death via XRCC1 activation.

Hyper-activation of the CK2/XRCC1 axis causes IPF fibroblasts to become resistant to cisplatin-induced apoptosis

To confirm our finding that the CK2/XRCC1 axis participates in protecting IPF fibroblasts from cisplatin-induced cell death via enhanced DNA repair, we next over-expressed XRCC1 in CK2 silenced IPF fibroblasts, and DNA damage and fibroblast viability were measured on collagen. As we expected, γH2AX/H2AX levels were significantly increased in the presence of CK2 siRNA while γH2AX/H2AX expression was reduced when XRCC1 was over-expressed in cisplatin treated IPF fibroblasts (Fig. 5a, upper lanes 3 and 2, lower). In contrast, compared to CK2 siRNA treated cells, γH2AX/H2AX expression remained low when CK2 silenced IPF fibroblasts were transfected with a construct over-expressing XRCC1 (Fig. 5a, upper lane 4, and lower). To further support the anti-apoptotic role of CK2-dependent XRCC1 activation, CK2 silencing decreased IPF fibroblast viability (Fig. 5b, lower orange bars) while the reconstitution of XRCC1 in CK2 silenced IPF cells increased viability in response to cisplatin as a function of time (Fig. 5b, lower orange and red boxes). Collectively, our results showed that abnormal activation of CK2 increases DNA repair activity via XRCC1 up-regulation, which causes IPF fibroblasts to have an apoptosis-resistant phenotype in response to cisplatin.
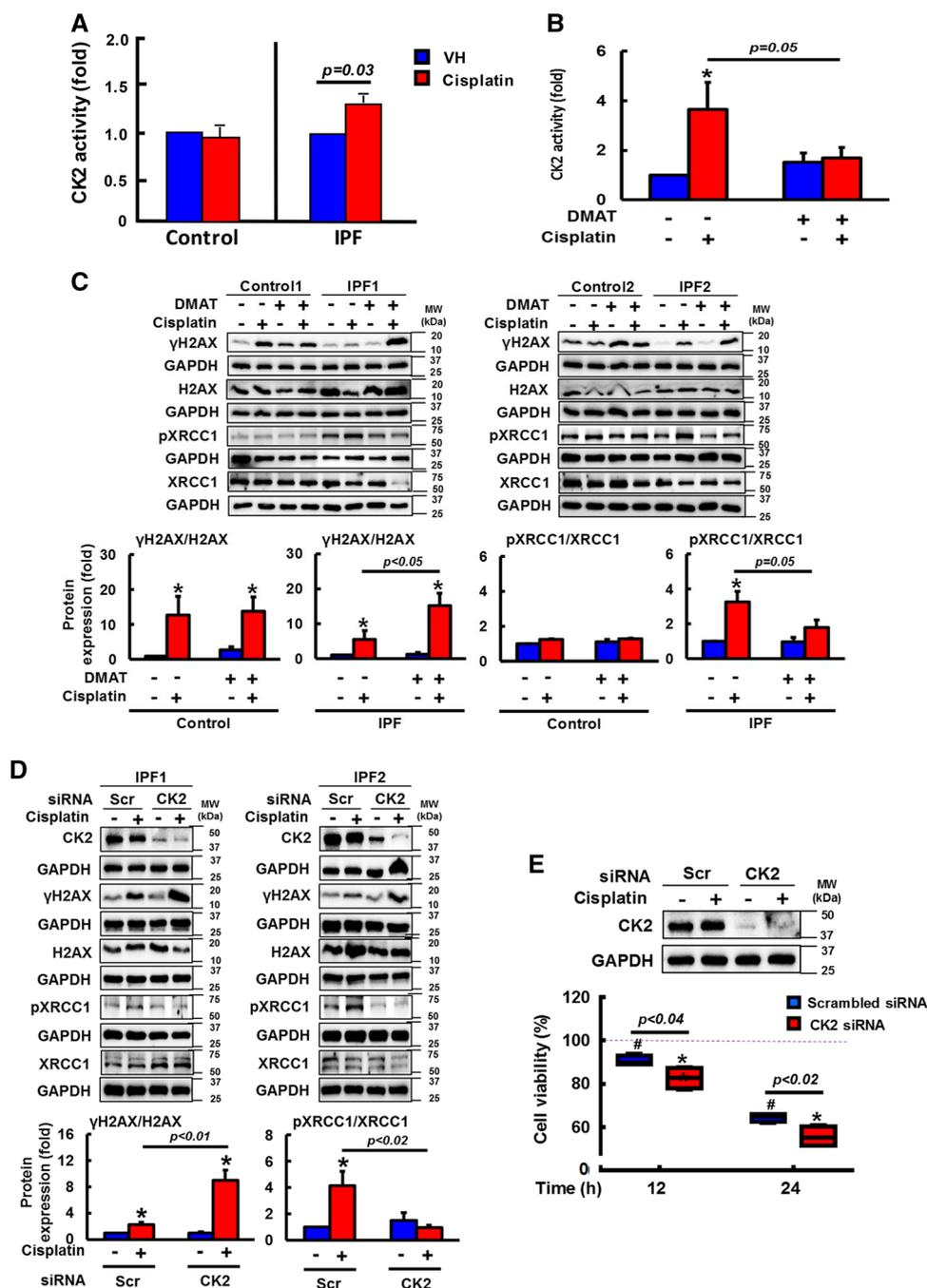
Discussion

The successful treatment of cancer patients with chemotherapy has been often hampered as a result of undesirable side effects. Among them, pulmonary toxicity is found in lung cancer patients treated with an anticancer chemotherapy agent cisplatin [17–19]. Cisplatin has been widely used for the treatment of various types of cancer such as bladder, head and neck, lung and ovarian cancers. Cisplatin is known to be effective in selectively promoting cancer cell death by crosslinking DNA. However, in spite of its established anti-cancer effects, there have been growing concerns that cisplatin treated patients have an increased risk of developing organ fibrosis including lung fibrosis [18, 19]. The emergence or the activation of fibrotic fibroblasts is particularly problematic for cancer

◀**Fig. 4** CK2 inhibition sensitizes IPF fibroblasts from cisplatin-induced cell death by the suppression of XRCC1 activity. **a** CK2 activity in 100 μM cisplatin treated control or IPF fibroblasts (n = 8, each) cultured on collagen was measured at 12 h. Values are presented in mean ± SEM of fold changes of CK2 activity compared to VH treated control or IPF fibroblasts set at onefold. **b** CK2 activity in IPF fibroblasts (n = 4) pre-treated with a 10 μM CK2 inhibitor DMAT were measured at 12 h in the presence or absence of 100 μM of cisplatin on collagen. Values are presented in mean ± SEM of fold changes of CK2 activity compared to VH treated IPF fibroblasts in the absence of cisplatin set at onefold. *Indicates the statistical significance of CK2 activity in cisplatin treated IPF fibroblasts compared to DMSO treated cells. $p < 0.05$. **c** *Upper*, representative γH2AX, total H2AX, pXRCC1, and total XRCC1 protein expression in control and IPF fibroblasts (n = 4 each) pre-treated with 10 μM DMAT at 12 h in the presence or absence of 100 μM cisplatin is shown. *Lower*, statistical analysis of γH2AX/H2AX and pXRCC1/XRCC1 protein levels in control and IPF fibroblasts under the same condition. Values are presented in mean ± SEM of fold changes of γH2AX/H2AX or pXRCC1/XRCC1 expression. VH treated control or IPF fibroblasts in the absence of cisplatin set at onefold. * indicates the statistical significance of γH2AX/H2AX or pXRCC1/XRCC1 in cisplatin or cisplatin and DMAT treated control or IPF fibroblasts compared to VH treated control or IPF fibroblasts. $p < 0.05$. **d** *Upper*, representative CK2, γH2AX, total H2AX, pXRCC1, and total XRCC1 protein expression in CK2 silenced IPF fibroblasts (n = 4) at 12 h in the presence or absence of 100 μM cisplatin. *Lower*, statistical analysis of γH2AX/H2AX and pXRCC1/XRCC1 protein levels in IPF fibroblasts under the same condition. Values are presented in mean ± SEM of fold changes of γH2AX/H2AX or pXRCC1/XRCC1 expression compared to VH treated IPF fibroblasts that were transfected with Scr siRNA set at onefold. *Indicates the statistical significance of γH2AX/H2AX in Scr or CK2 siRNA treated IPF fibroblasts compared to VH and Scr siRNA treated IPF fibroblasts. $p < 0.05$. **e** *Upper*, CK2 protein levels in IPF fibroblasts transfected with Scr or CK2 siRNA in the presence or absence of cisplatin at 12 h on collagen. *Lower*, cell viability in CK2 silenced IPF fibroblasts (n = 4) on collagen at 12 and 24 h in the presence or absence of 100 μM cisplatin. Values are presented in mean ± SEM of percentages of fibroblast viability compared to VH treated IPF fibroblasts that were transfected with Scr siRNA at 0 h set at 100%. # or *Indicates the statistical significance of cell viability in Scr or CK2 siRNA treated IPF fibroblasts at 12 and 24 h compared to VH and Scr siRNA treated IPF cells at 0 h. $p < 0.05$. IPF fibroblasts showing high cell viability and control cells showing low cell viability in response to cisplatin were used for these experiments

patients, and the pathological role of cancer-associated fibroblasts was previously studied [36, 37]. Cancer-associated fibroblasts are often perpetually activated and resistant to apoptosis inducing conditions including chemotherapy drugs, accelerating tumor progression [37, 38]. Interestingly, the pathological property seen in cancer-associated fibroblasts is also frequently found in IPF fibroblasts. These results imply that the cisplatin may trigger the fibrotic process as a result of persistent fibrotic fibroblasts, which in turn, accelerates tumor growth. IPF is characterized by the presence of apoptosis-resistant fibrotic fibroblasts that produce excessive amounts of a collagen rich extracellular matrix. Thus, we sought to investigate whether IPF fibroblasts elude cisplatin-induced genotoxic effects, which causes IPF fibroblasts to maintain a cell death-resistant property implicated in the development of lung fibrosis.

The DNA base excision repair (BER) plays an important role in repairing DNA damage caused by cisplatin and other platin compounds [15, 18]. XRCC1 is a key protein in the base excision repair and single-strand break repair (SSBR) pathways [39, 40] and associated with cisplatin-induced DNA repair [41]. Our results showed that there are two important molecular processes that protect IPF fibroblasts from cisplatin-induced cell death; (1) CK2 activity is aberrantly increased in cisplatin treated IPF fibroblasts, upregulating XRCC1 activity; (2) XRCC1-dependent DNA repair reduces cisplatin-induced genotoxic effects, maintaining intact DNA, which in turn, causes IPF fibroblasts to have an apoptosis-resistant phenotype. Thus, it is a feasible scenario that the presence (emergence) of highly viable fibrotic fibroblasts that repair DNA damage caused by cisplatin is associated with the development of fibrosis in cancer patients. To support our concept, several DNA damaging agents for the treatment of cancer patients are also known to be associated with the development of lung fibrosis. Bleomcyin is a well known anti-cancer agent to promote lung fibrosis [35, 42–44]. Interestingly, bleomycin is also known to generate DNA breaks, and bleomycin treatment increased non-IPF fibroblast cell death while IPF fibroblasts were resistant to bleomycin-induced cell death via enhanced DNA repair activity [11]. Since both cisplatin and bleomycin cause DNA breaks, the administration of combined bleomycin-cisplatin chemotherapy is known to worsen the outcomes [45, 46]. Radiation therapy is an additional example. Ionizing radiation is often used as primary or adjuvant treatment for cancer patients. A prior study showed that IPF fibroblasts cultured on collagen were resistant to ionizing radiation-induced cell death as a result of enhanced DNA repair activity [11]. These results further support the concept that the presence of cell death-resistant fibrotic fibroblasts in cancer patients during chemo- and/or radiotherapy that promotes DNA damage may accelerate the fibrotic process. Thus, monitoring the signs or symptoms of lung fibrosis before and/
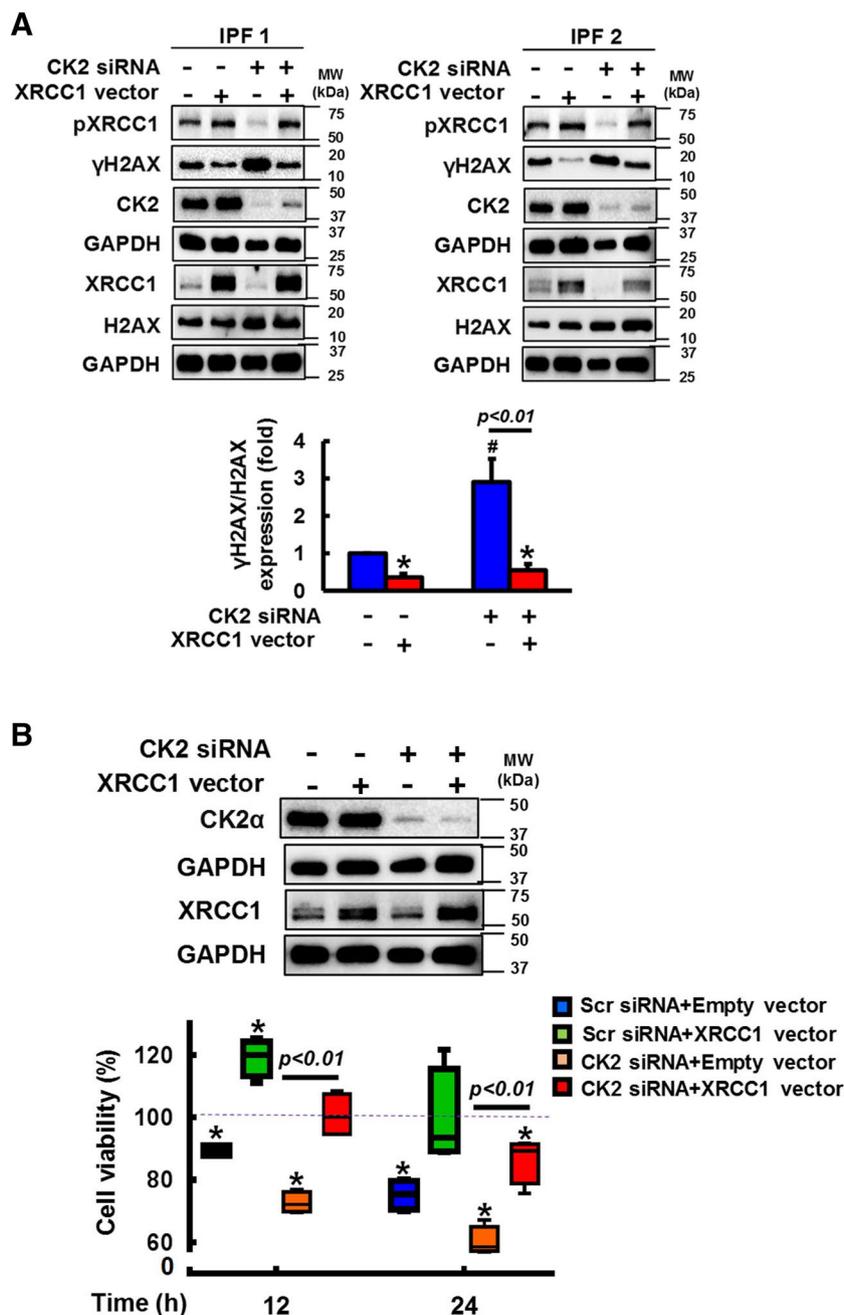
Fig. 5 IPF fibroblasts are resistant to cisplatin-induced cell death via CK2/XRCC1 activation. **a** *Upper*, representative images of CK2, γH2AX, total H2AX, pXRCC1 and total XRCC1 protein expression in CK2 silenced IPF fibroblasts (n=4) that were transfected with a vector over-expressing XRCC1 at 12 h in the presence of 100 μM cisplatin. *Lower*, statistical analysis of γH2AX/H2AX protein levels in IPF fibroblasts (n=4) under the same condition. Values are presented in mean ± SEM of fold changes of γH2AX/H2AX compared to Scr and empty vector transfected IPF cells set at onefold. #Indicates the statistical significance of γH2AX/H2AX in CK2 siRNA transfected IPF fibroblasts compared to Scr siRNA and empty vector transfected cells. *Indicates the statistical significance of γH2AX/H2AX in IPF cells transfected with a XRCC vector only or both CK2 siRNA and a XRCC1 vector compared to Scr siRNA and empty vector transfected

IPF cells. $p < 0.05$. **b** *Upper*, CK2α protein levels in CK2 siRNA transfected IPF fibroblasts over-expressing XRCC1 at 12 h on collagen in the presence of 100 μM cisplatin. GAPDH was used as a loading control. *Lower*, cell viability in CK2 siRNA treated IPF fibroblasts (n=4) overexpressing XRCC1 at 12 and 24 h in the presence of 100 μM cisplatin on collagen. Values are presented in mean ± SEM of percentages of fibroblast viability compared to Scr siRNA treated IPF cells that were transfected with an empty vector at 0 h set at 100%. *Indicates the statistical significance of cell viability of IPF fibroblasts transfected with Scr or CK2 siRNA with or without a construct over-expressing XRCC1 in the presence of cisplatin compared to that of an empty vector and Scr siRNA treated IPF fibroblasts at 0 h. $p < 0.05$

or during cisplatin treatment may be important to produce more effective outcomes, and that if necessary, anticancer agents other than cisplatin may minimize the risk of developing lung fibrosis.

Compliance with ethical standards

Disclosures Authors declare no competing financial interests.

References

1. Gay SE, Kazerooni EA, Toews GB, Lynch JP, Gross BH, Cascade PN, Spizarny DL, Flint A, Schork MA, Whyte RI, Popovich J, Hyzy R, Martinez FJ (1998) Idiopathic pulmonary fibrosis: predicting response to therapy and survival. Am J Respir Crit Care Med 157:1063–1072

2. Katzenstein AL, Myers JL (1998) Idiopathic pulmonary fibrosis: clinical relevance of pathologic classification. Am J Respir Crit Care Med 157:1301–1315

3. Ryu JH, Colby TV, Hartman TE (1998) Idiopathic pulmonary fibrosis: current concepts. Mayo Clin Proc 73:1085–1101

4. Coward WR, Saini G, Jenkins G (2010) The pathogenesis of idiopathic pulmonary fibrosis. Ther Adv Respir Dis 4:367–388

5. Kuhn C, McDonald JA (1991) The roles of the myofibroblast in idiopathic pulmonary fibrosis. Ultrastructural and immunohistochemical features of sites of active extracellular matrix synthesis. Am J Pathol 138:1257–1265

6. Im J, Kim K, Hergert P, Nho RS (2016) Idiopathic pulmonary fibrosis fibroblasts become resistant to Fas ligand-dependent apoptosis via the alteration of decoy receptor 3. J Pathol 240:25–37

7. Nho RS (2015) Alteration of aging-dependent MicroRNAs in idiopathic pulmonary fibrosis. Drug Dev Res 76:343–353

8. Im J, Kim K, Yhee JY, O'Grady SM, Nho RS (2016) Desensitization of idiopathic pulmonary fibrosis fibroblasts to Alternaria alternata extract-mediated necrotic cell death. Physiol Rep 4:e13020

9. Wilson MS, Wynn TA (2009) Pulmonary fibrosis: pathogenesis, etiology and regulation. Mucosal Immunol 2:103–121

10. Lawrence J, Nho R (2018) The role of the mammalian target of rapamycin (mTOR) in pulmonary fibrosis. Int J Mol Sci https://doi.org/10.3390/ijms19030778

11. Im J, Lawrence J, Seelig D, Nho RS (2018) FoxM1-dependent RAD51 and BRCA2 signaling protects idiopathic pulmonary fibrosis fibroblasts from radiation-induced cell death. Cell Death Dis 9:584

12. Nho RS, Hergert P (2014) IPF fibroblasts are desensitized to type I collagen matrix-induced cell death by suppressing low autophagy via aberrant Akt/mTOR kinases. PLoS ONE 9:e94616

13. Nho RS, Im J, Ho YY, Hergert P (2014) MicroRNA-96 inhibits FoxO3a function in IPF fibroblasts on type I collagen matrix. Am J Physiol Lung Cell Mol Physiol 307:L632–L642

14. Jamieson ER, Lippard SJ (1999) Structure, recognition, and processing of cisplatin-DNA adducts. Chem Rev 99:2467–2498

15. Dijt FJ, Fichtinger-Schepman AM, Berends F, Reedijk J (1998) Formation and repair of cisplatininduced adducts to DNA in cultured normal and repair-deficienthuman fibroblasts. Cancer Res 48:6058–6062

16. Dasari S, Tchounwou PB (2014) Cisplatin in cancer therapy: molecular mechanisms of action. Eur J Pharmacol 740:364–378

17. Guinee DG Jr, van Zee B, Houghton DC (1993) Clinically silent progressive renal tubulointerstitial disease during cisplatin chemotherapy. Cancer 71:4050–4054

18. Jordan P, Carmo-Fonseca M (2000) Molecular mechanisms involved in cisplatin cytotoxicity. Cell Mol Life Sci 57:1229–1235

19. Yuasa T, Yano R, Izawa T, Kuwamura M, Yamate J (2014) Calponin expression in renal tubulointerstitial fibrosis induced in rats by Cisplatin. J Toxicol Pathol 27:97–103

20. Ohe Y, Yamamoto S, Suzuki K, Hojo F, Kakinuma R, Matsumoto T, Ohmatsu H, Nishiwaki Y (2001) Risk factors of treatment-related death in chemotherapy and thoracic radiotherapy for lung cancer. Eur J Cancer 37:54–63

21. Sun C, Wei X, Fei Y, Su L, Zhao X, Chen G, Xu Z (2016) Mobile phone signal exposure triggers a hormesis-like effect in $Atm^{+/+}$ and $Atm^{-/-}$ mouse embryonic fibroblasts. Sci Rep 6:37423

22. Lee KY, Im JS, Shibata E, Dutta A (2017) ASF1a promotes non-homologous end joining repair by facilitating phosphorylation of MDC1 by ATM at double-strand breaks. Mol Cell 68:61–75.e5

23. Lan L, Nakajima S, Oohata Y, Takao M, Okano S, Masutani M, Wilson SH, Yasui A (2004) In situ analysis of repair processes for oxidative DNA damage in mammalian cells. Proc Natl Acad Sci USA 101:13738–13743

24. Wadey KS, Brown BA, Sala-Newby GB, Jayaraman PS, Gaston K, George SJ (2017) Protein kinase CK2 inhibition suppresses neointima formation via a proline-rich homeodomain-dependent mechanism. Vasc Pharmacol 99:34–44

25. Yun S, Vincelette ND, Knorr KL, Almada LL, Schneider PA, Peterson KL, Flatten KS, Dai H, Pratz KW, Hess AD, Smith BD, Karp JE, Hendrickson AE, Fernandez-Zapico ME, Kaufmann SH (2016) 4EBP1/c-MYC/PUMA and NF-κB/EGR1/BIM pathways underlie cytotoxicity of mTOR dual inhibitors in malignant lymphoid cells. Blood 127:2711–2722

26. Tian W, de la Rojo Vega M, Schmidlin CJ, Ooi A, Zhang DD (2018) Kelch-like ECH-associated protein 1 (KEAP1) differentially regulates nuclear factor erythroid-2-related factors 1 and 2 (NRF1 and NRF2). J Biol Chem 293:2029–2040

27. Olive PL, Banáth JP (2009) Kinetics of H2AX phosphorylation after exposure to cisplatin. Cytometry B Clin Cytom 76:79–90

28. Bonner WM et al (2008) GammaH2AX and cancer. Nat Rev Cancer 8:957–967

29. Rogakou EP, Pilch DR, Orr AH, Ivanova VS, Bonner WM (1998) DNA double-stranded breaks induce histone H2AX phosphorylation on serine 139. J Biol Chem 273:5858–5868

30. Sigurðsson HH, Olesen CW, Dybboe R, Lauritzen G, Pedersen SF (2015) Molecular cancer research. Constitutively active ErbB2 regulates cisplatin-induced cell death in breast cancer cells via pro- and antiapoptotic mechanisms. Mol Cancer Res 13:63–77

31. Taylor RM, Wickstead B, Cronin S, Caldecott KW (1998) Role of a BRCT domain in the interaction of DNA ligase III-alpha with the DNA repair protein XRCC1. Curr Biol 8:877–880

32. Xu W, Chen Q, Wang Q, Sun Y, Wang S, Li A, Xu S, Røe OD, Wang M, Zhang R, Yang L, Zhou J (2014) JWA reverses cisplatin resistance via the CK2-XRCC1 pathway in human gastric cancer cells. Cell Death Dis 5:e1551

33. Xu W, Wang S, Chen Q, Zhang Y, Ni P, Wu X, Zhang J, Qiang F, Li A, Røe OD, Xu S, Wang M, Zhang R, Zhou J (2014) TXNL1-XRCC1 pathway regulates cisplatin-induced cell death and

contributes to resistance in human gastric cancer. Cell Death Dis 5:e1055

34. Parsons JL, Dianova II, Finch D, Tait PS, Ström CE, Helleday T, Dianov GL (2010) XRCC1 phosphorylation by CK2 is required for its stability and efficient DNA repair. DNA Repair (Amst) 9: 835–841

35. Mills P, Husband J (1990) Computed tomography of pulmonary bleomycin toxicity. Semin Ultrasound CT MR 11:417–422

36. Sirica AE (2011) The role of cancer-associated myofibroblasts in intrahepatic cholangiocarcinoma. Nat Rev Gastroenterol Hepatol 9:44–54

37. Kharaishvili G, Simkova D, Bouchalova K, Gachechiladze M, Narsia N, Bouchal J (2014) The role of cancer-associated fibroblasts, solid stress and other microenvironmental factors in tumor progression and therapy resistance. Cancer Cell Int 14:41

38. Mao Y, Keller ET, Garfield DH, Shen K, Wang J (2013) Stromal cells in tumor microenvironment and breast cancer. Cancer Metastasis Rev 32:303–315

39. Thompson LH, West MG (2000) XRCC1 keeps DNA from getting stranded. Mutat Res 459:1–18

40. Campalans A, Marsin S, Nakabeppu Y, O'connor TR, Boiteux S, Radicella JP (2005) XRCC1 interactions with multiple DNA glycosylases: a model for its recruitment to base excision repair. DNA Repair 4:826–835

41. Zhang R, Niu Y, Zhou Y (2010) Increase the cisplatin cytotoxicity and cisplatin-induced DNA damage in HepG2 cells by XRCC1 abrogation related mechanisms. Toxicol Lett 192:108–114

42. Della Latta V, Cecchettini A, Del Ry S, Morales MA (2015) Bleomycin in the setting of lung fibrosis induction: from biological mechanisms to counteractions. Pharmacol Res 97:122–130

43. Lazo JS, Hoyt DG (1990) The molecular basis of interstitial pulmonary fibrosis caused by antineoplastic agents. Cancer Treat Rev 17:165–167

44. Hay J, Shahzeidi S, Laurent G (1991) Mechanisms of bleomycin-induced lung damage. Arch Toxicol 65:81–94

45. Rabinowits M, Souhami L, Gil RA, Andrade CA, Paiva HC (1990) Increased pulmonary toxicity with bleomycin and cisplatin chemotherapy combinations. Am J Clin Oncol 13:132–138

46. Brodsky A, Aparici I, Argeri C, Goldenberg D (1989) Stevens-Johnson syndrome, respiratory distress and acute renal failure due to synergic bleomycin-cisplatin toxicity. J Clin Pharmacol 29:821–823